AGU PUBLICATIONS

Geochemistry, Geophysics, Geosystems

RESEARCH ARTICLE

10.1002/2016GC006621

Key Points:

- Low precipitation/evaporation ratio in Lake Van region during MIS 4-2 deduced from algal and terrestrial plant biomarkers
- Coinciding increase of lipid hydrogen isotopic composition (δD) indicates changes in moisture availability and source
- High ACE index values due to low GDGT-0 concentrations reveal the presence of halophilic euryarchaeota

Supporting Information:

- Supporting Information S1

Correspondence to:
C. Schubert,
carsten.schubert@eawag.ch

Citation:
Randlett, M.-E., A. Bechtel, M. T. J. van der Meer, F. Peterse, T. Litt, N. Pickarski, O. Kwiecien, M. Stockhecke, B. Wehrli, and C. J. Schubert (2017), Biomarkers in Lake Van sediments reveal dry conditions in eastern Anatolia during 110.000–10.000 years B.P., *Geochem. Geophys. Geosyst.*, *18*, 571–583, doi:10.1002/2016GC006621.

Received 1 SEP 2016
Accepted 11 JAN 2017
Accepted article online 16 JAN 2017
Published online 15 FEB 2017

Biomarkers in Lake Van sediments reveal dry conditions in eastern Anatolia during 110.000–10.000 years B.P.

Marie-Eve Randlett[1,2], Achim Bechtel[3], Marcel T. J. van der Meer[4], Francien Peterse[2,5], Thomas Litt[6], Nadine Pickarski[6], Ola Kwiecien[7], Mona Stockhecke[8,9], Bernhard Wehrli[1,2], and Carsten J. Schubert[1,2]

[1]Eawag, Swiss Federal Institute of Aquatic Science and Technology, Department of Surface Waters – Research and Management, Kastanienbaum, Switzerland, [2]ETH Zurich, Institute of Biogeochemistry and Pollutant Dynamics, Zurich, Switzerland, [3]Chair in Petroleum Geology, Montanuniversität, Leoben, Austria, [4]NIOZ Royal Netherlands Institute for Sea Research and Utrecht University, Department of Marine Microbiology and Biogeochemistry, 't Horntje (Texel), Netherlands, [5]Department of Earth Sciences, Utrecht University, Utrecht, Netherlands, [6]Steinmann Institute of Geology, Mineralogy and Palaeontology, University of Bonn, Bonn, Germany, [7]Ruhr-Universität Bochum, Institut für Sediment- und Isotopengeologie, Bochum, Germany, [8]Eawag, Department of Surface Water - Research and Management, Dübendorf, Switzerland, [9]Large Lakes Observatory, University of Minnesota Duluth, Duluth, Minnesota, USA

Abstract Lipid biomarkers were analyzed in Lake Van sediments covering the last 600 ka, with a focus on the period between 110 and 10 ka, when a broad maximum in pore water salinity as a relict from the past suggests dry conditions. The occurrence and distribution of biomarkers indicative for terrestrial plants (long-chain *n*-alkane C_{29}), haptophyte algae (methyl alkenones C_{37}) and halophilic archaea (archaeol) all point toward a dry climate in Lake Van region during this time interval. The hydrogen isotopic composition of C_{29} *n*-alkanes (δD_{C29}) and C_{37} alkenones (δD_{C37}) is enriched between MIS 4 and MIS 2, which is interpreted as a decrease in the regional ratio of precipitation to evaporation. Similarly, the low abundance of the acyclic glycerol dialkyl glycerol tetraether GDGT-0 relative to archaeol, quantified by the Archaeol and Caldarchaeol Ecometric (ACE) is assumed to reflect the presence of halophilic euryarchaeota adapted to high salinity water. The climate around Lake Van appears in phase with the Yammouneh basin 800 km southwest and Lake Urmia 250 km southeast of Lake Van over the last two glacial periods. The results highlight the potential of combining ACE, δD_{C29}, and δD_{C37} for reconstructing salinity changes and regional precipitation to evaporation ratio from lake sediments.

1. Introduction

The availability of rainwater on land has had major effects on human migrations over the past two glacial-interglacial cycles in the eastern Mediterranean region [*Robinson et al.*, 2006; *Frumkin et al.*, 2011; *Rohling et al.*, 2013]. To reconstruct rainwater availability, well-dated terrestrial archives spanning several thousands of years are necessary. In the eastern Mediterranean, these notably include speleothems [*Bar-Matthews et al.*, 2003; *Almogi-Labin et al.*, 2009] and sediment records [*Bartov et al.*, 2003; *Gasse et al.*, 2011].

The sedimentary archive of Lake Van in eastern Anatolia offers a unique opportunity for reconstructing rainwater availability in the eastern Mediterranean region over the last 600 ka [*Litt et al.*, 2009]. Since Lake Van is endorheic, its water level is highly sensitive to the regional ratio of precipitation to evaporation (p/e ratio). This ratio is nowadays controlled by the Subtropical High Pressure Belt, resulting in dry conditions during summers, and moisture transport by midlatitude westerly winds predominating during spring and fall [*Alpert et al.*, 1990; *Sariş et al.*, 2010]. Over seasonal and decadal timescales, Lake Van water level fluctuations are on the order of a few centimeters to a few meters [*Kaden et al.*, 2010]. So far, past water level fluctuations of Lake Van have been reconstructed using inorganic tracers, such as the oxygen isotopic composition ($\delta^{18}O$) of authigenic calcite or the Mg/Ca ratio [*Landmann and Reimer*, 1996; *Wick et al.*, 2003]. This has revealed that Lake Van water levels fluctuated in the order of several tens of meters over the last glacial-interglacial transition, probably linked to latitudinal shifts of atmospheric circulation patterns [*Landmann et al.*, 1996]. Periods of higher water levels are further recognized and identified by radiometric dating of terraces found around the lake [*Kuzucuoğlu et al.*, 2010]. Lower lake levels were identified using seismic stratigraphy [*Cukur et al*., 2013]. In general, glacials are characterized by dry conditions, whereas interglacials were wetter over the last 600 ka [*Stockhecke et al*., 2014b]. In 2010, a 220 m long sediment record was obtained in the context of the ICDP project Paleovan, now allowing to investigate past regional water availability in the Lake Van region in more detail.

The pore water salinity profile for the last 110 ka suggest that dry conditions prevailed during the Last Glacial period (Y. Tomonaga et al., Porewater salinity reveals past lake-level changes in Lake Van, the Earth's largest soda lake, submitted to *Scientific Reports*, 2017). However, pore water can diffuse upward with time and hence the profile may not represent the original pore water profile. To validate the exceptionally dry climate conditions, we here analyzed a suite of lipid biomarkers in Lake Van sediments spanning the last 600 ka, with a focus on the period between 110 and 10 ka when pore water salinity values were high. Since lipids are incorporated into the insoluble phase of the sediment, the possibility of diffusion inherent to the pore water salinity signal is eliminated. The lipid biomarkers used here have a known biological source and a proven potential for reconstructing humidity in the catchment, salinity and p/e ratio. Long-chain *n*-alkanes (including $C_{27,\ 29,\ 31}$) are constituents of leaf waxes of terrestrial plants [*Eglinton and Hamilton*, 1967; *Jetter et al*., 2006]. Since meteoric water is used for lipid synthesis, the long-chain *n*-alkanes are recorders of the water cycle. The hydrogen isotope composition of leaf wax lipids (δD_{wax}) in lake-surface sediments is mainly linked to the hydrogen isotope composition of regional rainwater (δD_{rain}) [*Huang et al*., 2004; *Sachse et al*., 2004; *Hou et al*., 2008; *Polissar and Freeman*, 2010; *Garcin et al*., 2012], although in certain environments biosynthetic fractionation and eco-physiological aspects such as photosynthetic pathways (C_3 versus C_4) [*Chikaraishi and Naraoka*, 2003; *Smith and Freeman*, 2006] and evaporative D-enrichment of leafwater are dominant [*Kahmen et al*., 2013a; *Zech et al*., 2015]. As such, the stable hydrogen isotopic composition of leaf waxes (here, δD_{C29}) can be used to reconstruct past p/e ratios [e.g., *Sachse et al*., 2012] with higher values corresponding to arid conditions and low precipitation [e.g., *Schefuß et al*., 2005; *Tierney et al*., 2008, 2015; *Niedermeyer et al*., 2016].

Similarly, the hydrogen isotopic composition (here, δD_{C37}) of long-chain alkenones ($C_{37:2}$, $C_{37:3}$, $C_{37:4}$) that are biosynthesized by haptophyte algae thriving in Lake Van [*Randlett et al*., 2014] can be used for reconstructing salinity. Culture studies have shown that the δD_{C37} reflects the salinity-controlled H/D ratio in the water in which the alkenone-producing haptophytes live [*Schouten et al*., 2006; *Chivall et al*., 2014; *M'Boule et al*., 2014]. Measuring δD_{C37} values in sediments has resulted in salinity reconstructions for various locations of different geological age [*van der Meer et al*., 2007; *Kasper et al*., 2014; *Petrick et al*., 2015; *Simon et al*., 2015]. Finally, the glycerol dialkyl glycerol tetraether (GDGT) and archaeol found in the cell membranes of Archaea ubiquitous in water, sediments, soils, and peat bogs [*Schouten et al*., 2013] are used to reconstruct lake water salinity based on the Archaeol and Caldarchaeol (i.e. GDGT-0) Ecometric (ACE; equation (1)). This index is based on the assumption that the producers of GDGT-0 are suppressed under saline conditions [*Turich and Freeman*, 2011]. Organisms living under hypersaline conditions appear to produce only diphytanyl glycerol diethers (DGDs) including archaeol [*Teixidor et al*., 1993; *Kates*, 1996; *Grice et al*., 1998].

Using the occurrence and isotopic composition of these biomarkers, we here aim to provide an independent, continuous record of past hydroclimate variability in the Lake Van region, and to confirm the occurrence of extremely dry conditions between ca. 110–10 ka suggested by high pore water salinity values.

2. Regional Setting

Lake Van lies 1649 m above sea level (m.a.s.l.) in eastern Anatolia (Figure 1). The region is tectonically active and lies at the collision zone between the Arabian and the Eurasian plates [*Cukur et al*., 2016]. Today, Lake Van is endohreic with a maximal water depth of 450 m and a water volume of 600 km^3 [*Degens and Kurtman*, 1978; *Cukur et al*., 2014]. The water level is controlled by freshwater inputs (precipitation and river discharges) estimated between 2 and 4 $km^3\ a^{-1}$, as well as by evaporation estimated to 4 $km^3\ a^{-1}$ [*Degens and Kurtman*, 1978; *Reimer et al*., 2009]. The lake water is brackish with a salinity between 21.5 and 22.5 ‰, highly alkaline with a pH between 9.7 and 9.9 and contains sulfates with concentrations comparable to seawater [*Reimer et al*., 2009]. Bottom waters are less oxygenated (<50 μmol L^{-1}) than surface waters (> 200 μmol L^{-1}) and deep waters renewal occurs once every 6–23 years [*Kipfer et al*., 1994; *Kaden et al*., 2010].

The catchment covers approx. 16,000 km^2 and includes the Bitlis mountains massif as well as the Nemrut and the Süphan volcanos, which reach maximum altitudes of 4434 m.a.s.l. [*Degens and Kurtman*, 1978]. The

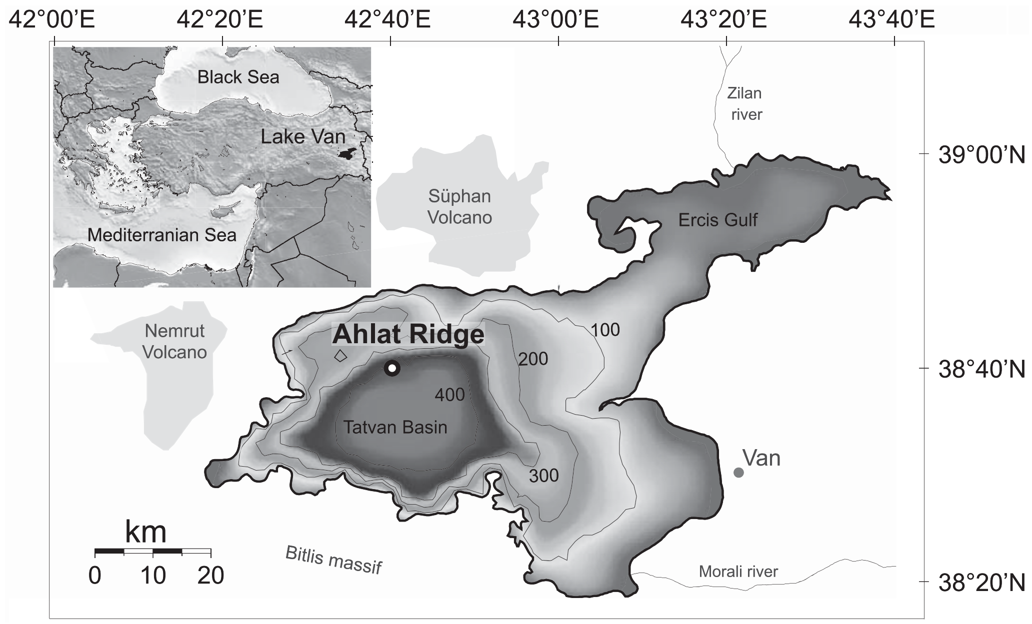

Figure 1. Geographical location and bathymetry of Lake Van. Modified from *Cukur et al.* [2013].

climate is continental with dry summers and precipitation carried through south-westerly winds in spring, autumn and winter [*van Zeist and Woldring*, 1978]. There is a strong gradient of annually precipitation in the catchment and the north-east region receives on average 300–400 mm, whereas the south-west region receives on average 600–800 mm [*van Zeist and Woldring*, 1978]. This is also reflected in the vegetation with the north-east region is characterized by high plateau steppe and oak-forest remnants, whereas the south-west region is characterized by a Kurdo-Zagrosian oak forest [*van Zeist and Woldring*, 1978; *Wick et al*., 2003].

The hydrogen stable isotopic composition of precipitation (δD_{precip}), temperature and precipitation amount data provided by *IAEA/WMO* [2014] are available for Erzurum (39°54'N, 41°16'E, 1758 m.a.s.l.) and Senyurt (40.20°N, 41.50°E, 2'210 m.a.s.l.) (Figure 1). These locations are considered representative of the Lake Van region, given their location on the eastern Anatolian plateau. Precipitation in Erzurum and Senyurt reaches maxima in spring (or at the beginning of summer) and in autumn. δD_{precip} in Erzurum and Senyurt displays a seasonal variability of about 120 ‰ (Figure 2). Higher δD_{precip} values are observed during the summer season. δD_{precip} seems more influenced by air temperatures than by the amount of precipitation. δD_{precip} of Erzurum is plotted against air temperature in Figure 2c.

3. Material and Methods

3.1. Sediment

3.1.1. Sampling

A 220 m long sediment record was drilled in summer 2010 at Ahlat Ridge (AR) (38°40'N 42°40'E) at a water depth of 350 m [*Litt et al*., 2012]. The composite profile covers approximately the past 600 ka or marine isotopic stages (MIS) 1 to 15 [*Stockhecke et al*., 2014a]. From this composite profile, a total of 93 samples were selected for lipid analyses based on their total organic carbon content (% TOC $\geq$ 1) and on the depth at which large climatic transitions were identified by preliminary pollen and X-ray fluorescence analyses. In order to recover the most recent (Holocene) sediments disturbed by the drilling operations of the drill core, a 1 m-long push core was additionally obtained in the vicinity of the AR drilling site. Four samples from this short core were used for lipid analyses. All samples were freeze-dried and homogenized before lipid extraction.

3.1.2. Age Model

The age model was constructed using climatostratigraphic alignment, varve chronology, tephrostratigraphy, argon-argon single-crystal dating, radiocarbon dating, magnetostratigraphy, and cosmogenic nuclides [*Stockhecke et al*., 2014a]. The presented aligned chronology is based on Greenland Ice Core Chronology

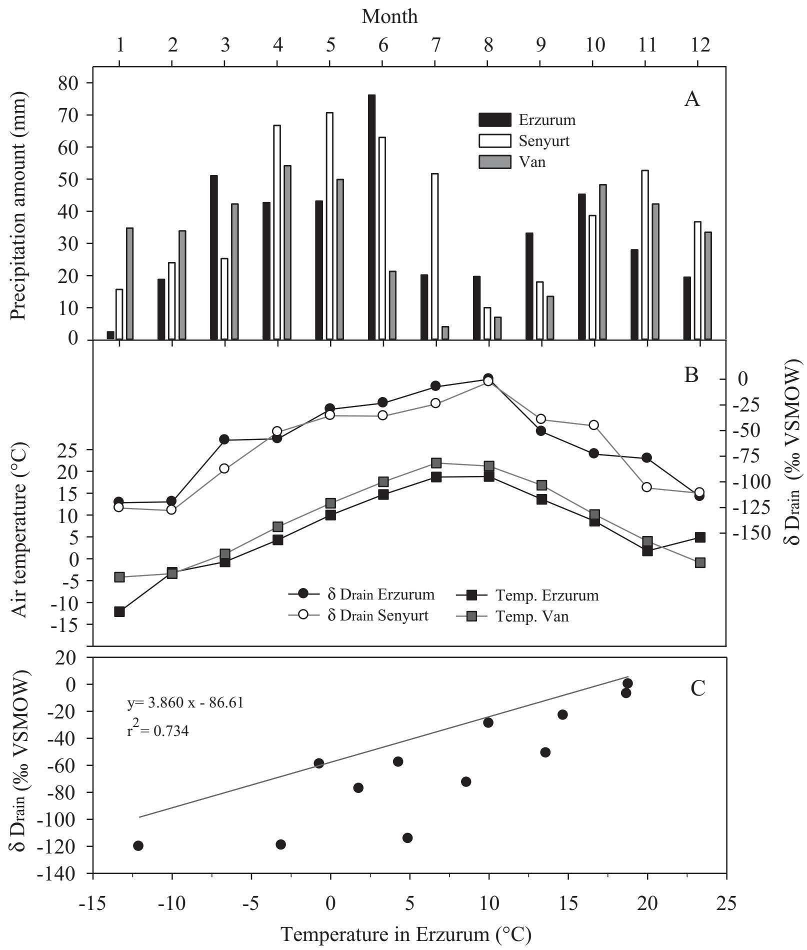

Figure 2. (a) Amount of precipitation (bars) and air temperature (line) over 1 year in Erzurum and in Senyurt [*IAEA/WMO*, 2014]. (b) Isotopic signature of precipitation over 1 year in Erzurum and in Senyurt. (c) Correlation between the isotopic composition of precipitation and temperature in Erzurum.

2005 (GICC05) [*NGRIPmembers*, 2004; *Steffensen et al*., 2008; *Svensson et al*., 2008; *Wolff et al*., 2010] from 0 to 116 ka, the speleothem-based synthetic Greenland record (GLT-syn) [*Barker et al*., 2011] for the interval 116–400 ka, and the same synthetic Greenland record but on the EDC timescale from Antarctic ice cores for 400 to 600 ka (GLT-syn) [*Barker et al*., 2011]. Eight geomagnetic tie points (from ~32 to ~250 ka), based on minima in the RPI record, and nine $^{40}Ar/^{39}Ar$ ages confirm the age model [*Stockhecke et al*., 2014a].

3.2. Lipid Biomarkers

3.2.1. Extraction and Purification

Lipids were extracted from 1 to 6 g of freeze-dried and homogenized sediment, with a mixture of 10 mL of dichloromethane (DCM) and methanol (MeOH) (7:3 v/v) in microwave teflon bombs for 2 min at 300 W and 5 min at 500 W. The total lipid extract (TLE) was transferred to a separatory funnel containing 20 mL of nanopure water with 5% NaCl to remove the salts. The lipids were extracted from the saline aqueous phase using 3 × 10 mL DCM and free elemental sulfur was eliminated with HCl preactivated copper powder. Fatty acids were released by saponification in 3 mL of 6% KOH in MeOH at 80°C for 3 h. The neutral lipids were recovered by extracting the KOH/MeOH with 3 × 1 mL hexane, then separated over a silica column (230–400 mesh Merck, 4 cm length, 0.6 cm diameter) into 3 fractions of various polarity using 4 mL of the following eluents: 1) 100% hexane; 2) hexane: DCM mixture (1:2 v/v) and 3) DCM: MeOH mixture (95: 5 v/v). The first fraction contained the long-chain *n*-alkanes, the second fraction collected the alkenones, and the third fraction contained the GDGTs and archaeol.

3.2.2. Quantification and Characterization

n-Alkanes and alkenones were identified on a gas chromatograph coupled to a mass spectrometer (GCMS-QP2010 Ultra, Shimadzu) and quantified on a gas chromatograph (GC, Shimadzu) using C_{36} *n*-alkane as an internal standard. A Restek Rxi-5ms 60 m column with an inner diameter of 0.32 mm and a film thickness of 0.25 μm was used. The GC oven temperature program was: 70°C to 130°C at 20°C/min, then to 320°C (held 20 min) at 4°C/min. A He carrier gas flow of 1.0 ml/min was used. Reproducibility based on triplicate analyses of selected samples was 3%. Two proxies that describe the origin of organic matter using *n*-alkane abundance were calculated in the following way [*Marzi et al*., 1993; *Bush and McInerney*, 2013]:

1. Average chain length (ACL) = $(\Sigma[C_i] \times i)/\Sigma[C_i]$ where i = carbon number ranges (*n*-alkanes, C_{23-33}), C_i=the concentration of the homologues containing i carbon atoms.
2. Carbon preference index (CPI) = 2 (odd $C_{23\text{-}31}$)/(even $C_{22\text{-}30}$ + even $C_{24\text{-}32}$)

A known amount of C_{46} GDGT standard was added to the third fraction, containing the GDGTs and archaeol [cf. *Huguet et al*., 2006]. The fraction was dissolved in hexane: isopropanol (99:1, v/v), and filtered over a 0.45 μm PTFE filter prior to analysis using high performance liquid chromatography/atmospheric pressure chemical ionization-mass spectrometry (HPLC/APCI-MS) on an Agilent 1260 Infinity series at ETH Zürich. HPLC/APCI-MS settings were according to *Schouten et al*. [2007], and separation was achieved with a Grace Prevail Cyano column (150 mm × 2.1 mm; 3 um), preceded by a guard column of the same material. Compounds were eluted isocratically with 90% A and 10% B for 5 min and then with a linear gradient to 18% B for 34 min with a flow rate of 0.2 ml/min, where A = hexane, and B = hexane: isopropanol (9:1, v/v). Selected ion monitoring of the $[M+H]^+$-ions was used to detect the different GDGTs, and quantification was achieved by calculating the area of their corresponding peaks in the chromatogram compared to that of the internal standard. Archaeol was analyzed in a separate run together with GDGT-0 and the C_{46} GDGT standard following the same method. The retention time of archaeol was determined by analyzing a 1,2-di-O-phytanyl-sn-glycerol standard from Avanti Lipids, Alabaster, AL, USA [cf. *Turich and Freeman*, 2011], and its relative response through time by injecting different mixtures of the archaeol and C_{46} GDGT standards. Regular reruns of selected samples on the HPLC at ETH show that the analytical error is < 0.01.

The ACE was calculated according to *Turich and Freeman* [2011]:

$$\mathrm{ACE}=(\mathrm{archaeol})/(\mathrm{archaeol}+\mathrm{GDGT}-0)\times 100 \tag{1}$$

3.2.3. Hydrogen and Carbon Stable Isotopic Composition of Hydrocarbon Biomarkers

Stable carbon and hydrogen isotope measurements on *n*-alkanes were performed using a Trace GC-Ultra gas chromatograph (GC) attached to a Thermo Fischer Delta-V isotope ratio mass spectrometer (irMS) via a combustion and high temperature reduction interface, respectively (GC Isolink, Thermo Fischer). The GC coupled to the irMS was equipped with a 30 m DB-5MS fused silica capillary column (i.d. 0.25 mm; 0.25 µm film thickness). The GC oven temperature was programmed from 70 to 300°C at a rate of 4°C/min followed by an isothermal period of 15 min. Helium was used as a carrier gas. The sample was injected splitless at 275°C. The temperature of the different reactors was set to 1030°C for stable carbon isotope analysis (combustion) and 1420°C for hydrogen isotope analysis (high temperature conversion). Analytical reproducibility (0.2 ‰ for $\delta^{13}C$; 2 ‰ for δD) was controlled by repeated measurements of *n*-alkane standard mixtures (Mixture C prepared by Arndt Schimmelmann, University of Indiana) and isotopic composition are reported in the δ notation relative to the international standards VPDB for carbon and VSMOW for hydrogen. Since the *n*-alkane C_{29} had the highest average concentration (~295 µg g_{sed}^{-1}) in all the samples, we show isotopic values only for this compound.

Stable H isotope measurements (δD_{C37}) on the C_{37} alkenones represent the integrated value for the alkenone compounds $MeC_{37:4}$, $MeC_{37:3}$, and $MeC_{37:2}$ [*van der Meer et al*., 2013]. δD_{C37} values were obtained by averaging duplicate analysis performed on a mass spectrometer (Thermo Electron DELTA$^+$XL). Alkenone hydrogen isotope analyses were carried out on a Thermo Finnigan DELTAPlus XL GC/TC/irMS. The temperature conditions of the GC increased from 70 to 145 °C at 20 °C min−1, then to 320 °C at 4 °C min−1, at which it was held isothermal for 13 min using an Agilent CP Sil-5 column (25m×0.32 mm) with a film thickness of 0.4 μm and 1mLmin−1 helium at constant flow. The thermal conversion temperature was set to 1425 °C. The alkenones were measured in four batches and the H^{3+} correction factor was determined daily and, although different for each batch, always 10 or lower and varying by less than 0.2 from day to day.

Isotope values for alkenones were standardized against pulses of H_2 monitoring gas, which was injected three times at the beginning and two times at the end of each run. A set of standard *n*-alkanes with known isotopic composition (Mixture B prepared by Arndt Schimmelmann, University of Indiana) was analyzed daily prior to each sample batch in order to monitor the system performance. Samples were only analyzed when the alkanes in Mix B had an average deviation from their off-line determined value of <5 ‰. Squalane was coinjected as an internal standard with each sample to monitor the precision of the alkenone isotope values and yielded an average δD value of -168.2 ‰ for all measurements, which compared favorably with its offline determined δD value of -170 ‰. Fractions containing the alkenones were analyzed at least in duplicate and reproducibility was generally 3‰ or lower.

4. Results

The records of δD_{C29}, δD_{C37}, and ACE index showed similar trends (Figure 3), and increased around 110 ka, although the exact onset of this increase is slightly different between each parameter.

δD_{C29} values ranged between -152 and -179‰ and increased around 100 ka. Relatively high δD_{C29} values (≥ -165‰) are observed between 90 and 30 ka, compared to other periods when δD_{C29} values were lower (<-165 ‰; Figure 3). The δD_{C37} values of the alkenones in the sediments varied during the last 600 ka from -178 to -125 ‰. Relatively high values were observed during stages 6, 4, 3 and 2, i.e., mainly during colder stages. The pore water salinity profile displayed a broad maximum (>25 ‰) between 70 and 15 ka, compared to other periods when pore water salinity values were lower ($<$ 25; Figure 3; (Tomonaga et al., submitted manuscript, 2017)). The ACE index varied between 0 and 78, and was highest between 90 and 15 ka (Figure 3).

5. Discussion

5.1. Hydroclimate of Eastern Anatolia

δD values of lipids derived from terrestrial plants (long-chain *n*-alkanes, *n*-alcohols, and *n*-alkanoic acids with more than 24 carbon atoms) extracted from lake-surface sediments along climatic gradients have yielded strong linear relationships with mean annual δD_{precip} values [*Huang et al*., 2004; *Sachse et al*., 2004; *Hou et al*., 2008; *Polissar and Freeman*, 2010; *Garcin et al*., 2012]. δD values of Lake Van sediment plant waxes should hence reflect the meteoric water isotopic composition. *Dansgaard* [1964] already described three main factors responsible for δD_{precip} values; (1) temperature, i.e. higher fractionation between vapor and rain during lower temperatures in the region of precipitation, leading to lower δD values at higher latitudes and higher altitudes, (2) length of moisture transport, i.e. lower δD_{precip} the longer the transport path, and (3) the amount effect, where more rainfall leads to stronger deuterium depletion. In general, the temperature effect is dominant in regions outside the tropics, whereas the amount effect is most prominent in tropical latitudes [*Bowen*, 2008]. Since Lake Van is not situated in a tropical zone, only the first two factors need to be considered for the interpretation of the δD record. Modern δD_{precip} values at Lake Van are positively correlated with seasonal temperature variations (-13 and 20°C, Figure 2), suggesting that modern δD_{precip} values in the Lake Van area are primarily controlled by temperature (Figure 2). However, in the sediment profile, the most enriched δD_{C29} values are observed during interstadials (MIS 5d-5a, i.e., colder times during interglacials) and cold glacial periods (MIS 4 and 2), making it unlikely that they reflect high temperatures during these intervals, so that other factors than temperature must have controlled the δD_{C29} values in the Lake Van region in the past. One of the contributing factors is that in general the rain had higher δD values during glacial times since isotopically "light" water was stored in the ice caps. However, based on the shifts in δ^{18}O of benthic foraminifera (global marine record) during MIS 2-4 in comparison to MIS 5c and the Holocene, the maximum effect of ice volume on δD of precipitation can be estimated to be in the range of 10 ‰ with heavier values during glacials. Since the observed shift in δD during MIS 2-4 is up to 25 ‰, the effect of ice volume can only be a part of the explanation. An additional factor could be that the source area of the moisture supplied to the Lake Van region may have changed in the past, inducing a change in δD_{precip} values. Indeed, within a radius of 800 km around Lake Van, moisture sources can vary between the eastern Mediterranean Sea, the Black Sea, and the Caspian Sea, corresponding to a variation in modern mean growing season δD_{precip} values of about 60‰ [*Terzer et al*., 2013]. In Lake Van sediments, the interval of high δD_{C29} values between MIS 5 and MIS 2 shows approximately 20–25 ‰ higher values than the average

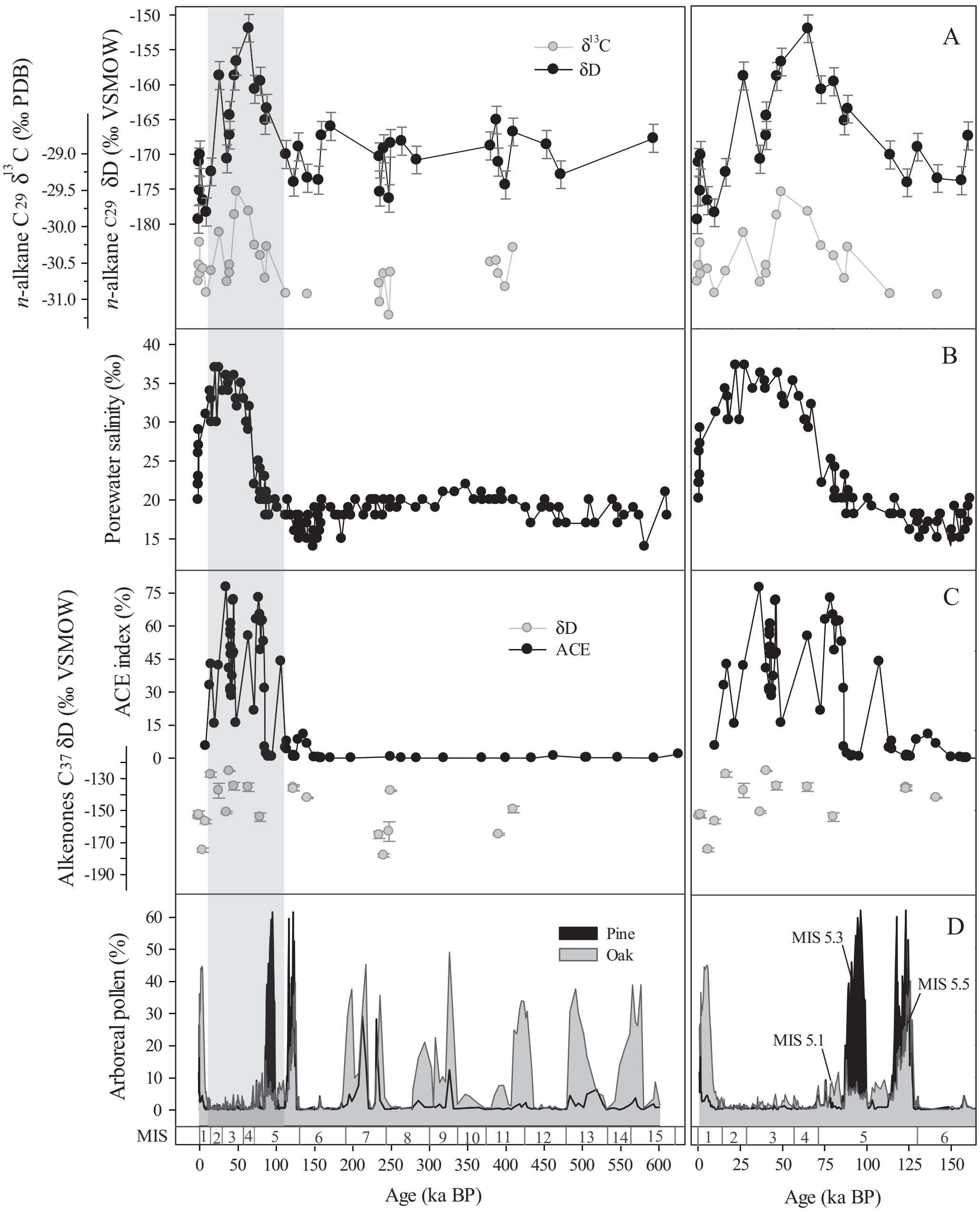

Figure 3. δD_{C29} and $\delta^{13}C_{C29}$ values of *n*-alkanes in (a) Lake Van Sediments, (b) pore-water salinity, (c) ACE index and δD_{C37} values, Summer green oak and pine pollen percentages [*Litt et al.*, 2014] versus age. Numbers located at the left bottom represent marine isotope stages (MIS). The shaded area on the left (approximately between 110 and 10 ka) highlights the time period during which δD_{C29}, pore-water salinity and the ACE index values are high.

δD_{C29} values observed over the last 600 ka (−169 ‰, Figure 3). Hence, a change of wind direction and temperature e.g., of relatively cooler winds from the eastern Mediterranean Sea to relatively warmer winds from northeastern Africa together with local changes of e.g., evapotranspiration is an additional plausible explanation.

Finally, δD_{C29} values are likely not influenced only by δD_{precip} but they may also depend on biological and ecological factors. Several studies have demonstrated a relationship between δD_{C29} and biosynthetic fractionation and/or eco-physiological aspects such as root depth, photosynthetic pathways (C_3 versus C_4), taxonomic classes (angiosperm versus gymnosperm) and growth forms (monocotyledon versus dicotyledon) [*Chikaraishi and Naraoka*, 2003; *Smith and Freeman*, 2006; *Kahmen et al.*, 2013b]. To verify if changes in vegetation composition and/or type had an influence on the δD_{C29} record between 110 and 10 ka around Lake Van, i.e. the time period with the highest resolution and significant changes, several other plant wax proxies were investigated. First, the average chain length (ACL) and the carbon preference index (CPI) of the *n*-alkanes [*Ficken et al*., 2000] was calculated. In Lake Van sediments the ACL is on average 29 (22–32) and the CPI ranges between 2 and 21 (average 7.4), which is typical for land plants [*Bray and Evans*, 1961; *Kolattukudy*, 1970]. Hence, the main source of *n*-alkanes, i.e. terrestrial plants can be assumed constant between 110 and 10 ka and can thus be correlated with the pollen signal. During the last glacial period, the vegetation is mainly composed of open steppe types, as indicated by the dominating occurrence of *Artemisia and Chenopodiaceae*. The increase of summer-green oak pollen during interstadials (108–87 and 85–78 ka, MIS 5c and MIS 5a) implies temporary warmer and/or more humid conditions [*Pickarski et al*., 2015a], although this is not so well resolved in the lower resolution biomarker profile. The carbon stable isotopic composition ($\delta^{13}C$) of the *n*-alkanes is another indicator for vegetation changes, as C_3 plants have $\delta^{13}C$ values of around -34.7 ‰, whereas values of C_4 plant waxes are typically higher, i.e. around -21.4 ‰ [*Castaeda et al*. 2009]. The $\delta^{13}C$ values of C_{29} *n*-alkanes in Lake Van sediments varied only marginally, i.e. between -32 and -29 ‰ throughout the past 600 ka (Figure 3). When only considering the period 110 - 10 ka, the range of variation is even smaller ($\pm$ 1.5 ‰). This relatively small $\delta^{13}C$ variation reflects a maximum contribution of C_4 plants of $<$12%. Hence, the minor shifts in vegetation type over the length of the core will have had only a negligible effect on the δD_{C29} record.

On the other side the linear relationship between $\delta^{13}C$ and δD of the long-chain *n*-alkanes can be interpreted as a stomatal constraint on leaf gas-exchange mediated by water supply rather than a change in plant type. Deuterium enrichment of leaf water through evapotranspiration, a mechanism occurring in sub arid regions [*Kahmen et al*., 2013a; *Kahmen et al*., 2013b] and along a humidity gradient [*Zech et al*., 2015] has been shown to be an important mechanism for leaf wax deuterium enrichment in certain areas. Evaporative deuterium enrichment, which may have occurred in the leaf and/or in the soil of Lake Van region, would be in agreement with other proxies (ACE index, salinity) indicating a dry climate. Moreover, the linear correlation between $\delta^{13}C$ and δD of terrestrial plant long-chain *n*-alkanes C_{29} and C_{31} are observed in the Lake Van sediment record (r^2=0.62 and 0.58, respectively) hints to the above mentioned evapotranspiration affecting simultaneously carbon ($^{13}C/^{12}C$) and hydrogen (D/H) isotope fractionations. Since under dry conditions, certain plants close their stomata to avoid losing water, which affects CO_2 exchange, basically limiting the pool of available CO_2 for biosynthesis resulting in reduced carbon isotope fractionation [*Farquhar et al*., 1989]. Carbon isotope fractionation therefore decreases with a reduction in water availability [*Diefendorf et al*., 2010]. To summarize, combined $\delta^{13}C$ and δD *n*-alkane data suggest a period of strong aridity in Lake Van area starting around 110 ka in accordance with the pollen profile (Figure 3).

5.2. Lake Van Salinity

5.2.1. Alkenone δD

Whereas the C_{29} *n*-alkanes reflect the conditions in the watershed around the lake, alkenones represent the conditions of the water column. Relatively higher δD_{C37} values were observed mainly during colder stages. The trend of the δD_{C37} record is similar to that of δD_{C29} from ~160 ka onward (Figure 3), especially during the transition from MIS 6 to MIS 5 (Figure 3, right). Interestingly, the records of δD_{C29} and δD_{C37} appear unrelated before 160 ka (Figure 3, left).

As previously revealed by fossil DNA analyses, the composition of haptophyte species in Lake Van varied over time [*Randlett et al*., 2014]. Whereas a variety of operational taxonomic units (OTU) namely LV_1, 3, 5 and 6 were present in samples of ages 267 ka and 239 ka, a dominant OTU LV_1 was detected in more recent samples (104 ka, 75.7 ka, 47.2 ka, 40.7 ka, 4.17 ka, 1.67 ka and 0.74 ka). The very light δD_{C37} (-178 ‰) measured at 240 ka is close to the sample at 239 ka where the haptophyte species LV_6 was detected. Large differences in hydrogen isotope fractionation have been reported for more coastal species (e.g., Isochrysis spp) and more open ocean species (e.g., Emiliania huxleyi [*M'Boule et al*., 2014]) and, although, all these OTUs are relatively closely related to each other and more closely related to Isochrysis spp than E. huxleyi a species effect on hydrogen isotope fractionation cannot be excluded for some of the observed differences. Further research on these more freshwater species in the future could clarify possible species effects for Lake Van. Since δD_{C37}, δD_{C29} and pore water salinity profiles are similar during the past 110 to 10 ka and evaporation increases salinity and lead therefore to deuterium enrichment, it is reasonable to assume a highly evaporative environment of Lake Van during this period.

Although the trend of both signals is similar, it seems that the δD_{C29} values lead the δD_{C37} values (see supporting information), i.e., changes occur earlier in the *n*-alkane profile. This is especially evident from 90 ka on toward the Holocene and indicates that climatic changes occurring in the region are first recorded by land plants before algae derived biomarkers are affected. However, a higher sample resolution is needed in the future to confirm this trend.

5.2.2. ACE Index

The ACE index in Lake Van varies between 0.1 and 77.6. It is normally below 5 before 88 ka with some higher vales around 146 to 132 ka and 110 to 107 ka. The ACE is primarily driven by GDGT-0 concentrations since those vary more widely (1.4 to 19,000 ng g_{sed}^{-1}) than those of archaeol (0.3 to 220 ng g_{sed}^{-1}, Figure 4). GDGT-0 concentrations are notably low (<100 ng g_{sed}^{-1}) between 90 and 15 ka, except for one data point at 82 ka. Archaeol concentrations were always below 6.3 ng g_{sed}^{-1} for ages >160 ka, but become higher toward modern times. Archaeol is known to occur also in methanogenic archaea, however since Lake Van has only low methane concentrations in the bottom water (<300 nM), we rule out a stronger influence of methanogenic archaea to the archaeol profile. Also GDGT-0/crenarchaeol is always < 2, indicating no significant contribution of methanogens to the GDGT-producing community [cf. *Blaga et al.*, 2009].

Lake Van is brackish today (salinity of 22), however, the pore water salinity record indicates that the lake was more saline (salinity of > 35) in the past. Lake water salinity started increasing at 75 ka, and reached a maximum around 30 ka (Tomonaga et al., submitted manuscript, 2017). This maximum correlates with erosional features displayed in the seismic profile, which indicates a minimum lake water level of about 145 m below the current lake level at that time [*Cukur et al.*, 2013; Tomonaga et al., submitted manuscript, 2017]. Such dramatic water level changes would go along with salinity variations as reflected by the pore water record and the ACE index. Hence, the ACE index does record salinity changes in Lake Van although the salinities that were reached are at the lower end of the calibration by *Turich and Freeman* [2011]. Instead of responding linearly and quantitatively to salinity changes through time, the ACE index might have responded only in a binary way with low values (i.e. no archaeol from halophiles) indicating fresh(er) water conditions versus high values indicating the presence of halophiles at higher salinity. Once the salinity in Lake Van exceeded a certain threshold, which seems to be around 20 ‰ based on the salinity pore-water profile, the presence of halophilic euryarchaeota raised archaeol concentrations and induced high ACE index values. Thus, the aforementioned arid conditions deduced from the isotopic signals in the Lake Van region correspond to more saline lake water recorded by the ACE index. Altogether, the covariation of all proxy records indicates that the Lake Van region experienced a very dry climate during the last 110 ka, most likely due to a subtle change in the precipitation/evaporation ratio [*Stockhecke et al.*, 2016]. Further support for dry conditions comes from pollen studies. Here an oak steppe-forest during the climate optimum at 129 to 124 ka and a more coniferous dominated forest at 124 to 111.5 ka was replaced by steppic herbaceous plants leading to arid desert-steppe vegetation in Eastern Anatolia from 75 ka to 12 ka [*Litt et al.*, 2014; *Pickarski et al.*, 2015a, 2015b].

For comparison, we have included Figure 5 which shows the PC1, the first principal component of a Principal Component Analysis using a suite of high-resolution proxies reflecting lake level changes of Lake Van

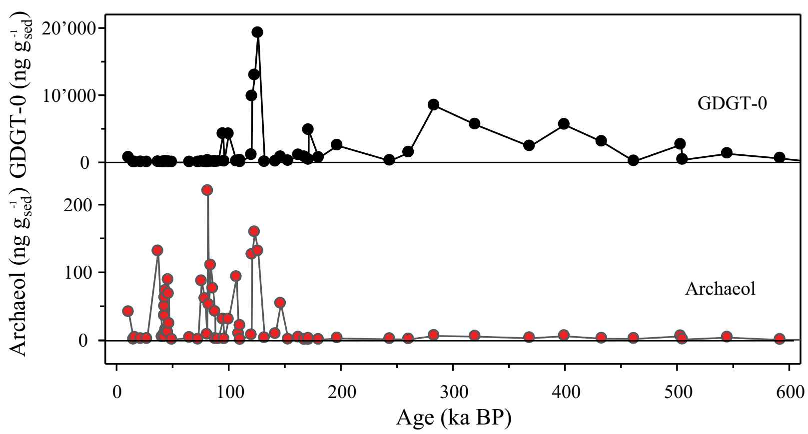

Figure 4. Temporal variation of GDGT-0 and archaeol concentrations in Lake Van sediment core.

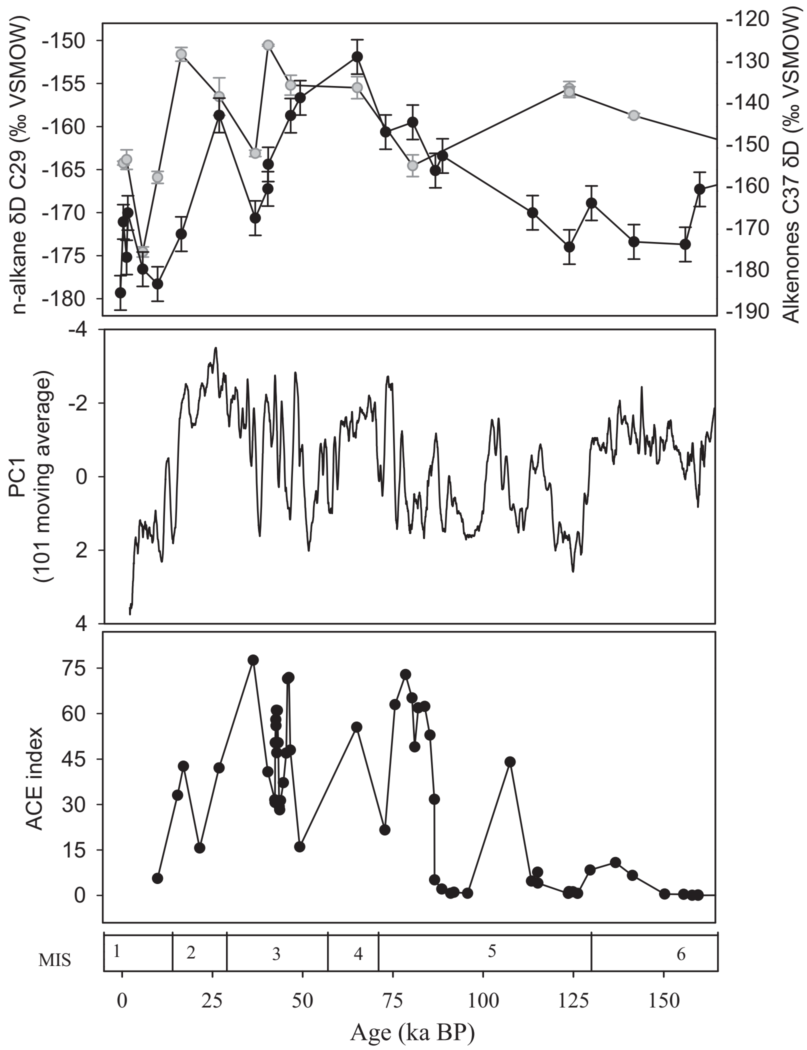

Figure 5. δD_{C29} values of *n*-alkanes, δD_{C37} of alkenones and the ACE index values in Lake Van sediments. Additionally, the hydroclimatic high-resolution reconstruction based on a suite of proxy records (PC1, negative: dry, positive: wet) is shown [*Stockhecke et al*., 2016].

[*Stockhecke et al*., 2016], the isotopic values of δD_{C29} and δD_{C37}, and the ACE index. The PC1 interpreted as proxy of hydroclimatic variability in the Eastern Mediterranean shows fluctuations that are related to both orbital-scale and millennial-scale variability over the last 350 ka [*Stockhecke et al*., 2016]. The high resolution that is reached with PC1 shows some fluctuations that did not show up in our proxies due to lower sampling. The PC1 shows additionally that the Lake Van region although in general dry underwent wet periods during all Dansgaard-Oeschger interstadials over the last 110 ka.

5.3. Comparison With Regional Records (Lake Urmia and Yammouneh Basin)

Lake Urmia and Yammouneh basin are located approximately 250 km southeast and 800 km southwest of Lake Van, respectively. Proxy records from these lakes (lithofacies, pollen, carbonate oxygen isotope analyses, and aquatic pollen) revealed that the Last Glacial (MIS 4-2) period was equally dry and even more arid than MIS 6 [*Gasse et al*., 2011; *Stevens et al*., 2012]. Lake Van proxy records support these trends, so that the arid conditions were prevailing in a larger area than only the Lake Van catchment. This also indicates that all three regions were likely influenced by the same shifts in the climate system.

5.4. Drivers of Lake Van Climate Change

Dry conditions deduced from our proxies between MIS 5d and MIS 2 can be linked to 100 ka timescale processes, affecting both global Eastern Mediterranean (EM) and regional Lake Van climate. Large atmospheric patterns responsible for drought conditions on the 100 ka timescale in the Eastern Mediterranean (EM) include an atmospheric response to orographic forcing (Laurentide and Eurasian ice-sheets), an anomalous low pressure system, and an advection of dry air from northeastern Africa [*Stockhecke et al*., 2016]. The latter process, which was dominant during MIS 4 to MIS 2 in the EM may have been coupled with a more local climatic process. A likely trigger for such a local phenomenon is a southward extension of the Siberian High Pressure System (SHPS), a system nowadays centered north of the Lake Van region and characterized by cold and dry air originating from the interior of the Eurasian continent. This mechanism was proposed to explain dry conditions in the Lake Van region during glacial periods [*Cagatay et al*., 2014]. Besides, several studies point toward an exceptionally large east Siberian ice sheet during MIS 4 [*Baumann et al*., 1995; *Svendsen et al*., 2004; *Krinner et al*., 2011], which may have been the cause for a temporarily southward extension of the SHPS, bringing cool and dry air to the Lake Van region, causing the observed aridity.

During MIS 4–2, temperature drops in the Mediterranean Sea were correlated to six Heinrich Events that occurred within 40 ka in the North Atlantic [*Martrat et al*., 2004; *Rodrigues et al*., 2011; *Girone et al*., 2013]. A combination of records of TOC, $CaCO_3$, arboreal pollen, Si, and potassium in Lake Van sediments that are available in high resolution, and transient earth system modeling experiments showed that a dry climate in the EM could be induced by Dansgaard-Oeschger (DO) cycles through weaker Atlantic Meridional Overturning Circulation (AMOC) and massive anti-cyclonic circulation anomalies [*Stockhecke et al*., 2016].

6. Conclusion and Outlook

In conclusion, proxies from the Lake Van record indicate a coherent evolution of the climate in eastern Anatolia: the period 110–10 ka was exceptionally dry, although intercalated humid periods were identified in higher resolution profiles [*Stockhecke et al*., 2016]. δD_{C29} and δD_{C37} profiles display relatively high values during that time interval indicating that evaporation exceeded precipitation. High ACE index values during this time interval are linked to the presence of halophilic euryarchaeota in the water column of Lake Van and support a high salinity due to high evaporation. Despite the low resolution, the proxy record based on terrestrial plants (δD_{C29}) leads that of algae derived δD_{C37}, indicating that the lake water column needed at least several hundreds of years to adapt to the arid conditions in the catchment. A comparison with continental records at proximity such as the Yammouneh basin and the Lake Urmia shows that Lake Van region is in phase in terms of water availability over the last two glacial periods.

Acknowledgments
We thank the PALEOVAN team for support during data collection and data sharing; Aysegül Feray Meydan and Deniz Cukur for their indispensable help during the field campaign, Mete Orhan, Mehmet Sahin and Münip Kanan from the ship's crew for their strong commitment and the IODP Core Repository staff in Bremen for their help during the sampling party. All data presented in this study can be found in the supporting information excel file. Any other inquiries are welcomed by the corresponding author. The PALEOVAN drilling campaign was financially supported by the International Continental Scientific Drilling Program (ICDP), the Deutsche Forschungsgemeinschaft (DFG), the Swiss National Science Foundation (SNF grants 200020_143340, 20FI21_124972 and 200021_124981) and the Scientific and Technological Research Council of Turkey (Tübitak). FP acknowledges ETH Fellowship (FEL-36 11-1) and NWO-VENI (863.13.016) and MTJvdM acknowledges NWO-VIDI (864.09.011) for funding.

References

Almogi-Labin, A., M. Bar-Matthews, D. Shriki, E. Kolosovsky, M. Paterne, B. Schilman, A. Ayalon, Z. Aizenshtat, and A. Matthews (2009), Climatic variability during the last 90 ka of the southern and northern Levantine Basin as evident from marine records and speleothems, *Quat. Sci. Rev.*, *28*(25–26), 2882–2896.

Alpert, P., B. U. Neeman, and Y. Shay-El (1990), Climatological analysis of Mediterranean cyclones using ECMWF data, *Tellus, Ser. A*, *42*(1), 65–77.

Barker, S., G. Knorr, R. L. Edwards, F. Parrenin, A. E. Putnam, L. C. Skinner, E. Wolff, and M. Ziegler (2011), 800,000 years of abrupt climate variability, *Science*, *334*(6054), 347–351.

Bar-Matthews, M., A. Ayalon, M. Gilmour, A. Matthews, and C. J. Hawkesworth (2003), Sea–land oxygen isotopic relationships from planktonic foraminifera and speleothems in the Eastern Mediterranean region and their implication for paleorainfall during interglacial intervals, *Geochim. Cosmochim. Acta 67*(17), 3181–3199.

Bartov, Y., S. L. Goldstein, M. Stein, and Y. Enzel (2003), Catastrophic arid episodes in the Eastern Mediterranean linked with the North Atlantic Heinrich events, *Geology*, *31*(5), 439–442.

Baumann, K. H., K. S. Lackschewitz, J. Mangerud, R. F. Spielhagen, T. C. W. Wolfwelling, R. Henrich, and H. Kassens (1995), Reflection of Scandinavian ice-sheet fluctuations in Norwegian sea sediments during the past 150,000 years, *Quat. Res.*, *43*(2), 185–197.

Blaga, C., G.-J. Reichart, O. Heiri, and J. Sinninghe Damsté (2009), Tetraether membrane lipid distributions in water-column particulate matter and sediments: A study of 47 European lakes along a north–south transect, *J. Paleolimnol.*, *41*(3), 523–540.

Bowen, G. J. (2008), Spatial analysis of the intra-annual variation of precipitation isotope ratios and its climatological corollaries, *J. Geophys. Res.*, *113*, D05113, doi:10.1029/2007JD009295.

Bray, E. E., and E. D. Evans (1961), Distribution of n-paraffins as a clue to recognition of source beds, *Geochim. Cosmochim. Acta*, *22*(1), 2–15.

Bush, R. T., and F. A. McInerney (2013), Leaf wax n-alkane distributions in and across modern plants: Implications for paleoecology and chemotaxonomy, *Geochim. Cosmochim. Acta*, *117*, 161–179.

Cagatay, M. N., N. Ogretmen, E. Damci, M. Stockhecke, U. Sancar, K. K. Eris, and S. Ozeren (2014), Lake level and climate records of the last 90 ka from the Northern Basin of Lake Van, eastern Turkey, *Quat. Sci. Rev.*, *104*, 97–116.

Castañeda, I.S., S. Mulitza, E. Schefuß, R. A. Lopes dos Santos, J. S. Sinninghe Damsté, and S. Schouten (2009), Wet phases in the Sahara/Sahel region and human migration patterns in North Africa, *Proc. Natl. Acad. Sci. U. S. A.*, *106*, 20159e20163.

Chikaraishi, Y. and H. Naraoka (2003), Compound-specific delta D-delta C-13 analyses of n-alkanes extracted from terrestrial and aquatic plants, *Phytochemistry*, *63*(3), 361–371.

Chivall, D., D. M'Boule, D. Sinke-Schoen, J. S. Sinninghe Damsté, S. Schouten, and M. T. J. van der Meer (2014), The effects of growth phase and salinity on the hydrogen isotopic composition of alkenones produced by coastal haptophyte algae, *Geochim. Cosmochim. Acta*, *140*, 381–390.

Cukur, D., F. Demirel-Schluter, E. Demirbag, C. Imren, F. Niessen, M. Toker, and G. PaleoVan-Working (2013), Sedimentary evolution of Lake Van (Eastern Turkey) reconstructed from high-resolution seismic investigations, *Int. J. Earth Sci.*, *102*(2), 571–585.

Cukur, D., S. Krastel, H.-U. Schmincke, M. Sumita, M. N. Çağatay, A. F. Meydan, E. Damci, and M. Stockhecke (2014), Seismic stratigraphy of Lake Van, eastern Turkey, *Quat. Sci. Rev.*, *104*, 63–84.

Cukur, D., et al. (2016), Structural characteristics of the Lake Van Basin, eastern Turkey, from high-resolution seismic reflection profiles and multibeam echosounder data: Geologic and tectonic implications, *Int. J. Earth Sci.*, *106*, 239–253.

Dansgaard, W. (1964), Stable isotopes in precipitation, *Tellus*, *16*(4), 436–468.

Degens, E. T., and F. Kurtman (1978), *The Geology of Lake Van*, MTA Press, Ankara.

Diefendorf, A. F., K. E. Mueller, S. L. Wing, P. L. Koch, and K. H. Freeman (2010), Global patterns in leaf 13C discrimination and implications for studies of past and future climate, *Proc. Natl. Acad. Sci. U. S. A.*, *107*(13), 5738–5743.

Eglinton, G. and R. J. Hamilton (1967), Leaf epicuticular waxes, *Science*, *156*(3780), 1322–1335.

Farquhar, G. D., J. R. Ehleringer, and K. T. Hubick (1989), Carbon Isotope Discrimination and Photosynthesis, *Annu. Rev. Plant Physiol. Plant Mol. Biol.*, *40*(1), 503–537.

Ficken, K. J., B. Li, D. L. Swain, and G. Eglinton (2000), An n-alkane proxy for the sedimentary input of submerged/floating freshwater aquatic macrophytes, *Org. Geochem.*, *31*(7–8), 745–749.

Frumkin, A., O. Bar-Yosef, and H. P. Schwarcz (2011), Possible paleohydrologic and paleoclimatic effects on hominin migration and occupation of the Levantine Middle Paleolithic, *J. Hum. Evol.*, *60*(4), 437–451.

Garcin, Y., V. F. Schwab, G. Gleixner, A. Kahmen, G. Todou, O. Séné, J.-M. Onana, G. Achoundong, and D. Sachse (2012), Hydrogen isotope ratios of lacustrine sedimentary n-alkanes as proxies of tropical African hydrology: Insights from a calibration transect across Cameroon, *Geochim. Cosmochim. Acta*, *79*, 106–126.

Gasse, F., L. Vidal, A. L. Develle, and E. Van Campo (2011), Hydrological variability in the Northern Levant: A 250 ka multiproxy record from the Yammouneh (Lebanon) sedimentary sequence, *Clim. Past*, *7*(4), 1261–1284.

Girone, A., P. Maiorano, M. Marino, and M. Kucera (2013), Calcareous plankton response to orbital and millennial-scale climate changes across the Middle Pleistocene in the western Mediterranean, *Palaeogeogr. Palaeoclimatol. Palaeoecol.*, *392*, 105–116.

Grice, K., S. Schouten, A. Nissenbaum, J. Charrach, and J. S. Sinninghe Damsté (1998), Isotopically heavy carbon in the C21 to C25 regular isoprenoids in halite-rich deposits from the Sdom formation, Dead Sea Basin, Israel, *Org. Geochem.*, *28*(6), 349–359.

Hou, J., W. J. D'Andrea, and Y. Huang (2008), Can sedimentary leaf waxes record D/H ratios of continental precipitation? Field, model, and experimental assessments, *Geochim. Cosmochim. Acta*, *72*(14), 3503–3517.

Huang, Y. S., B. Shuman, Y. Wang, and T. Webb (2004), Hydrogen isotope ratios of individual lipids in lake sediments as novel tracers of climatic and environmental change: A surface sediment test, *J. Paleolimnol.*, *31*(3), 363–375.

Huguet, C., E. C. Hopmans, W. Febo-Ayala, D. H. Thompson, J. S. S. Damste, and S. Schouten (2006), An improved method to determine the absolute abundance of glycerol dibiphytanyl glycerol tetraether lipids, *Org. Geochem.*, *37*(9), 1036–1041.

IAEA/WMO (2014), *Global Network of Isotopes in Precipitation, The GNIP Database*, Erzurum, Turkey, IAEA Publ., Vienna.

Jetter, R., L. Kunst, and A. L. Samuels (2006), Composition of plant cuticular waxes, in *Annual Plant Reviews,* vol. 23, *Biology of the Plant Cuticle*, edited by M. Riederer and C. Müller, pp. 145–181, Blackwell, Oxford, U. K.

Kaden, H., F. Peeters, A. Lorke, R. Kipfer, Y. Tomonaga, and M. Karabiyikoglu (2010), Impact of lake level change on deep-water renewal and oxic conditions in deep saline Lake Van, Turkey, *Water Resour. Res.*, *46*, W11508, doi:10.1029/2009WR008555.

Kahmen, A., B. Hoffmann, and D. Sachse (2013a), Leaf water deuterium enrichment shapes leaf wax n-alkane δD values of angiosperm plants II: Observational evidence and global implications, *Geochim. Cosmochim. Acta*, *111*, 50–63.

Kahmen, A., E. Schefuß, S. K. Arndt, L. A. Cernusak, J. B. West, and D. Sachse (2013b), Leaf water deuterium enrichment shapes leaf wax n-alkane δD values of angiosperm plants I: Experimental evidence and mechanistic insights, *Geochim. Cosmochim. Acta*, *111*, 39–49.

Kasper, S., M. T. J. van der Meer, A. Mets, R. Zahn, J. S. Sinninghe Damsté, and S. Schouten (2014), Salinity changes in the Agulhas leakage area recorded by stable hydrogen isotopes of C37 alkenones during Termination I and II, *Clim. Past*, *10*(1), 251–260.

Kates, M. (1996), Structural analysis of phospholipids and glycolipids in extremely halophilic archaebacteria, *J. Microbiol. Methods*, *25*(2), 113–128.

Kipfer, R., W. Aeschbach-Hertig, H. Baur, M. Hofer, D. M. Imboden, and P. Signer (1994), Injection of mantle type helium into Lake Van (Turkey), the clue for quantifying deep water renewal, *Earth Planet. Sci. Lett.*, *125*(1), 357–370.

Kolattukudy, P. (1970), Plant waxes, *Lipids*, *5*(2), 259–275.

Krinner, G., B. Diekmann, F. Colleoni, and G. Stauch (2011), Global, regional and local scale factors determining glaciation extent in Eastern Siberia over the last 140,000 years, *Quat. Sci.Rev.*, *30*(7–8), 821–831.

Kuzucuoğlu, C., et al. (2010), Formation of the Upper Pleistocene terraces of Lake Van (Turkey), *J. Quat Sci.*, *25*(7), 1124–1137.

Landmann, G. and A. Reimer (1996), Climatically induced lake level changes at Lake Van, Turkey, during the Pleistocene/Holocene transition, *Global Biogeochem Cycles*, *10*(4), 797–808.

Landmann, G., G. Lemcke, and S. Kempe (1996), Dating Late Glacial abrupt climate changes in the 14,570 yr long continuous varve record of Lake Van, Turkey, *Palaeogeogr. Palaeoclimatol. Palaeoecol.*, *122*(1-4), 107–118.

Litt, T., S. Krastel, M. Sturm, R. Kipfer, S. Örcen, G. Heumann, S. O. Franz, U. B. Ülgen, and F. Niessen (2009), PALEOVAN, International Continental Scientific Drilling Program (ICDP), site survey results and perspectives, *Quat. Sci. Rev.*, *28*(15-16), 1555–1567.

Litt, T., et al. (2012), 500,000 Years of Environmental History in Eastern Anatolia: The PALEOVAN Drilling Project, *Sci. Drill. Rep.*, Copernicus Gesellschaft mbH, Göttingen, *14*, pp. 18–29.

Litt, T., N. Pickarski, and G. Heumann (2014), A 600,000 years long continental pollen record from Lake Van, Eastern Anatolia (Turkey), *Quat. Sci. Rev.*, *104*, 30–41.

Martrat, B., J. O. Grimalt, C. Lopez-Martinez, I. Cacho, F. J. Sierro, J. A. Flores, R. Zahn, M. Canals, J. H. Curtis, and D. A. Hodell (2004), Abrupt temperature changes in the Western Mediterranean over the past 250,000 years, *Science*, *306*(5702), 1762–1765.

Marzi, R., B. E. Torkelson, and R. K. Olson (1993), A revised carbon preference index, *Org. Geochem.*, *20*(8), 1303–1306.

M'Boule, D., D. Chivall, D. Sinke-Schoen, J. S. Sinninghe Damsté, S. Schouten, and M. T. J. van der Meer (2014), Salinity dependent hydrogen isotope fractionation in alkenones produced by coastal and open ocean haptophyte algae, *Geochim. Cosmochim. Acta*, *130*, 126–135.

NGRIPmembers (2004), High-resolution record of Northern Hemisphere climate extending into the last interglacial period, *Nature*, *431*, 147–151.

Niedermeyer, E. M., M. Forrest, B. Beckmann, A. L. Sessions, A. Mulch, and E. Schefuß (2016), The stable hydrogen isotopic composition of sedimentary plant waxes as quantitative proxy for rainfall in the West African Sahel, *Geochim. Cosmochim. Acta*, *184*, 55–70.

Petrick, B. F., E. L. McClymont, F. Marret, and M. T. J. van der Meer (2015), Changing surface water conditions for the last 500 ka in the Southeast Atlantic: Implications for variable influences of Agulhas leakage and Benguela upwelling, *Paleoceanography*, *30*, 1153–1167, doi:10.1002/2015PA002787.

Pickarski, N., O. Kwiecien, D. Langgut, and T. Litt (2015a), Vegetation and environmental changes during the last interglacial in eastern Anatolia (Turkey), a new high-resolution pollen record from Lake Van, *Palaeogeogr. Palaeoclimatol. Palaeoecol.*, *435*, 145–158.

Pickarski, N., O. Kwiecien, M. Djamali, and T. Litt (2015b), Abrupt climate and vegetation variability of eastern Anatolia during the last glacial, *Clim. Past*, *11*(11), 1491–1505.

Polissar, P. J., and K. H. Freeman (2010), Effects of aridity and vegetation on plant-wax delta D in modern lake sediments, *Geochim. Cosmochim. Acta*, *74*(20), 5785–5797.

Randlett, M.-E., M. J. L. Coolen, M. Stockhecke, N. Pickarski, T. Litt, C. Balkema, O. Kwiecien, Y. Tomonaga, B. Wehrli, and C. J. Schubert (2014), Alkenone distribution in Lake Van sediment over the last 270 ka: Influence of temperature and haptophyte species composition, *Quat. Sci. Rev.*, *104*, 53–62.

Reimer, A., G. Landmann, and S. Kempe (2009), Lake Van, Eastern Anatolia, hydrochemistry and history, *Aquat. Geochem.*, *15*(1), 195–222.

Robinson, S. A., S. Black, B. W. Sellwood, and P. J. Valdes (2006), A review of palaeoclimates and palaeoenvironments in the Levant and Eastern Mediterranean from 25,000 to 5000 years BP: Setting the environmental background for the evolution of human civilisation, *Quat. Sci. Rev.*, *25*(13–14), 1517–1541.

Rodrigues, T., A. H. L. Voelker, J. O. Grimalt, F. Abrantes, and F. Naughton (2011), Iberian Margin sea surface temperature during MIS 15 to 9 (580–300 ka), Glacial suborbital variability versus interglacial stability, *Paleoceanography*, *26*, PA1204, doi:10.1029/2010PA001927.

Rohling, E. J., K. M. Grant, A. P. Roberts, and J. C. Larrasoana (2013), Paleoclimate variability in the Mediterranean and Red Sea Regions during the Last 500,000 years implications for hominin migrations, *Curr. Anthropol.*, *54*, S183–S201.

Sachse, D., J. Radke, and G. Gleixner (2004), Hydrogen isotope ratios of recent lacustrine sedimentary n-alkanes record modern climate variability, *Geochim. Cosmochim. Acta*, *68*(23), 4877–4889.

Sachse, D. (2012), Molecular paleohydrology: Interpreting the hydrogen-isotopic composition of lipid biomarkers from photosynthesizing organisms, *Annu. Rev. Earth Planet. Sci.*, *40*(1), 221–249.

Sariş, F., D. M. Hannah, and W. J. Eastwood (2010), Spatial variability of precipitation regimes over Turkey, *Hydrol. Sci. J.*, *55*(2), 234–249.

Schefuß, E., S. Schouten, and R. R. Schneider (2005), Climatic controls on central African hydrology during the past 20,000 years, *Nature*, *437*(7061), 1003–1006.

Schouten, S., J. Ossebaar, K. Schreiber, M. V. M. Kienhuis, G. Langer, A. Benthien, and J. Bijma (2006), The effect of temperature, salinity and growth rate on the stable hydrogen isotopic composition of long chain alkenones produced by Emiliania huxleyi and Gephyrocapsa oceanica, *Biogeosciences*, *3*(1), 113–119.

Schouten, S., C. Huguet, E. C. Hopmans, M. V. M. Kienhuis, and J. S. S. Damste (2007), Analytical methodology for TEX86 paleothermometry by high-performance liquid chromatography/atmospheric pressure chemical ionization-mass spectrometry, *Anal. Chem.*, *79*(7), 2940–2944.

Schouten, S., E. C. Hopmans, and J. S. S. Damste (2013), The organic geochemistry of glycerol dialkyl glycerol tetraether lipids: A review, *Org. Geochem.*, *54*, 19–61.

Simon, M. H., X. Gong, I. R. Hall, M. Ziegler, S. Barker, G. Knorr, M. T. J. van der Meer, S. Kasper, and S. Schouten (2015), Salt exchange in the Indian-Atlantic Ocean Gateway since the Last Glacial Maximum: A compensating effect between Agulhas Current changes and salinity variations?, *Paleoceanography*, *30*, 1318–1327, doi:10.1002/2015PA002842.

Smith, F. A. and K. H. Freeman (2006), Influence of physiology and climate on δD of leaf wax n-alkanes from C3 and C4 grasses, *Geochim. Cosmochim. Acta*, *70*(5), 1172–1187.

Steffensen, J. P., et al. (2008), High-resolution greenland ice core data show abrupt climate change happens in few years, *Science*, *321*(5889), 680–684.

Stevens, L., M. Djamali, V. Andrieu-Ponel, and J.-L. de Beaulieu (2012), Hydroclimatic variations over the last two glacial/interglacial cycles at Lake Urmia, Iran, *J. Paleolimnol.*, *47*(4), 645–660.

Stockhecke, M., O. Kwiecien, L. Vigliotti, T. Litt, N. Pickarski, H.-U. Schmincke, and N. Catagay (2014a), Chronostratigraphy of the 600 ka old continental record of Lake Van (Turkey), *Quat. Sci. Rev.*, *104*, 8–17.

Stockhecke, M., M. Sturm, I. Brunner, H.-U. Schmincke, M. Sumita, O. Kwiecien, D. Cukur, and F. Anselmetti (2014b), Sedimentary evolution and environmental history of Lake Van (Turkey) over the past 600, 000 years, *Sedimentology*, *61*(6), 1830–1861.

Stockhecke, M., A. Timmermann, R. Kipfer, G. H. Haug, O. Kwiecien, T. Friedrich, L. Menviel, T. Litt, N. Pickarski, and F. S. Anselmetti (2016), Millennial to orbital-scale variations of drought intensity in the Eastern Mediterranean, *Quat. Sci. Rev.*, *133*, 77–95.

Svendsen, J. I., et al. (2004), Late Quaternary ice sheet history of northern Eurasia, *Quat. Sci. Rev.*, *23*(11–13), 1229–1271.

Svensson, A., et al. (2008), A 60 000 year Greenland stratigraphic ice core chronology, *Clim. Past*, *4*(1), 47–57.

Teixidor, P., J. O. Grimait, J. J. Pueyo, and F. Rodriguez-Valera (1993), Isopranylglycerol diethers in non-alkaline evaporitic environments, *Geochim. Cosmochim. Acta*, *57*(18), 4479–4489.

Terzer, S., L. I. Wassenaar, L. J. Araguás-Araguás, and P. K. Aggarwal (2013), Global isoscapes for δ18O and δ2H in precipitation: Improved prediction using regionalized climatic regression models, *Hydrol. Earth Syst. Sci.*, *17*(11), 4713–4728.

Tierney, J. E., J. M. Russell, Y. Huang, J. S. S. Damsté, E. C. Hopmans, and A. S. Cohen (2008), Northern hemisphere controls on tropical Southeast African climate during the past 60,000 years, *Science*, *322*(5899), 252–255.

Tierney, J. E., C. C. Ummenhofer, and P. B. deMenocal (2015), Past and future rainfall in the Horn of Africa, *Sci. Adv.*, *1*(9), e1500682.

Turich, C., and K. Freeman (2011), Archaeal lipids record paleosalinity in hypersaline systems, *Org. Geochem.*, *42*(9), 1147–1157.

van der Meer, M. T. J., M. Baas, W. I. C. Rijpstra, G. Marino, E. J. Rohling, J. S. S. Damste, and S. Schouten (2007), Hydrogen isotopic compositions of long-chain alkenones record freshwater flooding of the Eastern Mediterranean at the onset of sapropel deposition, *Earth Planet. Sci. Lett.*, *262*(3-4), 594–600.

van der Meer, M. T. J., A. Benthien, J. Bijma, S. Schouten, and J. S. Sinninghe Damsté (2013), Alkenone distribution impacts the hydrogen isotopic composition of the C37:2 and C37:3 alkan-2-ones in Emiliania huxleyi, *Geochim. Cosmochim. Acta*, *111*, 162–166.

van Zeist, W., and H. Woldring (1978), A postglacial pollen diagram from Lake Van in east Anatolia, *Rev. Palaeobot. Palynol.*, *26*(1–4), 249–276.

Wick, L., G. Lemcke, and M. Sturm (2003), Evidence of Lateglacial and Holocene climatic change and human impact in eastern Anatolia: High resolution pollen, charcoal, isotopic and geochemical records from the laminated sediments of Lake Van, Turkey, Holocene, *13*(5), 665–675.

Wolff, E. W., J. Chappellaz, T. Blunier, S. O. Rasmussen, and A. Svensson (2010), Millennial-scale variability during the last glacial: The ice core record, *Quat. Sci. Rev.*, *29*(21-22), 2828–2838.

Zech, M., R. Zech, K. Rozanski, G. Gleixner, and W. Zech (2015), Do n-alkane biomarkers in soils/sediments reflect the dD isotopic composition of precipitation? A case study from Mt. Kilimanjaro and implications for paleoaltimetry and paleoclimate research, *Isotopes Environ. Helath Stud.*, *51*(4), 508–524.